Atmospheric Water Vapor Transport in NCEP–NCAR Reanalyses: Comparison with River Discharge in the Central United States*

William J. Gutowski Jr.,[+,#] Yibin Chen,[#] and Zekai Ötles[#]

ABSTRACT

The authors extract the water transport produced by the National Centers for Environmental Prediction reanalysis for a 10-yr period, 1984–93, and compare its convergence into two river basins with an independent dataset, river discharge (streamflow). Analysis focuses on two basins in the United States, the Upper Mississippi and the Ohio–Tennessee Basins, where the relatively high density of routine upper-air observations might be expected to give the reanalysis its closest rendition of the actual water transport. Over periods of several years, water input by the atmosphere should match water output from these basins in streamflow. However, in both basins an imbalance between the two with biases with respect to streamflow approaching 40% is found. The accuracy attributed to river discharge measurements averaged over several years and the apparent lack of significant multiyear storage in the basins lead us to conclude that the bias is largely an inaccuracy in the atmospheric transport. Temporal variability of atmospheric input and streamflow output shows somewhat better correspondence, with statistically significant correlations occurring for both basins on interannual and several-day timescales. The overall behavior suggests that the temporal variability of water transport depicted by the reanalysis can be used to gain insight into the actual variability of atmospheric transport, at least for well-observed regions such as the United States.

1. Introduction

Constructing a quantitative picture of water's cycling through its major reservoirs on our planet is a complex, challenging puzzle involving scientists of many disciplines. At present, we have only a rough, qualitative understanding of the earth's large-scale hydrologic cycle (National Research Council 1991). However, water is a critical element of the earth's climate system, so a quantitative understanding of the water cycle is greatly needed. The importance of constructing this quantitative understanding is underscored by the high priority the World Meteorological Organization has given to the Global Energy and Water Experiment (GEWEX; Chahine 1992), which is coordinating numerous water cycle research projects worldwide.

In this paper, we examine a quantitative depiction of one part of the water cycle, atmospheric water vapor transport. For a land region, this transport is critical because it links the local water cycle to the rest of the world. In this context, the most important part of the transport is its net input, or convergence, of water vapor into the region. Over suitably long periods, the horizontal flow of water vapor into a land region by atmospheric transport is balanced by the flow of water out of the region, primarily in rivers. Thus long-term fluctuations of atmospheric circulation affect fluctuations of stream outflow, which is generally a response to atmospheric forcing (Guetter and Georgakakos 1993). This expected relationship forms the basis of our analysis.

Water cycle studies for climate ideally would include uniform, multiyear observations of the day-to-day state of the atmosphere. In many previous studies, atmospheric water vapor divergence calculations were

*Iowa Agriculture and Home Economics Journal Paper No. 17131.
[+]Department of Agronomy, Iowa State University, Ames, Iowa.
[#]Department of Geological and Atmospheric Sciences, Iowa State University, Ames, Iowa.
Corresponding author address: Dr. William J. Gutowski Jr., Dept. of Geological and Atmospheric Sciences, Dept. of Agronomy, 3021 Agronomy, Iowa State University, Ames, IA 50011.
E-mail: gutowski@iastate.edu
In final form 31 March 1997.

based on rawinsonde measurements (e.g., Rasmusson 1967, 1968; Rosen et al. 1979a,b; Peixoto et al. 1981; Savijarvi 1988), which are available at irregularly spaced locations; other studies used gridded operational analysis (e.g., Roads et al. 1994; Chen et al. 1996b). However, operational analyses are subject to periodic alterations in operational procedures. These alterations can affect climatological computations such as water vapor transport, unless one restricts computations to relatively short periods in which the analysis system is unchanging. The U.S. National Centers for Environmental Prediction (NCEP) and the National Center for Atmospheric Research are performing a reanalysis of the atmosphere, reusing global weather observations collected over the past 40 yr as input into the contemporary computer tools that analyze the state of the atmosphere every 6 h (Kalnay and Jenne 1991; Kalnay et al. 1996). The reanalysis is applying a uniform procedure over the entire period from 1957 to the present, giving scientists one of the highest quality databases available for studying the earth's climate and its variability.

Observing water vapor well for climate study is difficult (Elliott and Gaffen 1991), which may temper expectations for the insight the reanalysis can provide into the hydrologic cycle. Part of this difficulty is due to measurement limitations inherent in even the most accurate, routinely used instruments, rawinsondes (e.g., Pratt 1985; Wade 1994). Also, atmospheric water vapor exhibits substantial variability on relatively small horizontal and vertical scales (e.g., Houze and Hobbs 1982; Starr and Melfi 1991; Iselin and Gutowski 1997), thus impeding the ability of typical observation networks to capture water vapor's three-dimensional distribution. The analysis scheme itself could introduce errors into analyzed water vapor. For example, the underlying forecast model may tend to evolve its hydrologic cycle toward a model, rather than real-world climatology (e.g., Donner and Rasch 1989 and references therein). These factors raise doubts about the quality of water vapor transport computed from atmospheric analyses. Indeed, Trenberth and Guillemot (1995) have suggested that even a state-of-the-art reanalysis may be deficient in this regard, although in observation-rich areas deficiencies may be minimized. Higgins et al. (1996) find general large-scale agreement in the moisture fluxes produced by two different reanalyses but regional differences.

We assess the accuracy of water vapor transport produced by the NCEP reanalysis by comparing its convergence in selected regions over multiyear periods with river discharge from these regions. We focus on two regions in the United States where we might expect the density of routine operational observations to yield one of the most accurate depictions of atmospheric water vapor in the reanalysis.

2. Methodology and data

a. Water balance equations

We examine water vapor transport using the budget equations for water in the atmosphere and the ground. The budget equation for vertically integrated atmospheric water vapor can be written (Peixoto and Oort 1992)

$$\frac{\partial P_\mathrm{W}}{\partial \mathrm{t}} = C - (P - E). \tag{1}$$

Here, P_w is the atmospheric precipitable water,

$$P_\mathrm{W} = \frac{1}{g}\int_0^{\mathrm{p_{sfc}}} q\,\mathrm{d}p, \tag{2}$$

where g is gravitational acceleration, q is specific humidity, p is pressure, and $\mathrm{p_{sfc}}$ is surface pressure. Also in (1), P is precipitation, E is evaporation, and C is horizontal convergence of vertically integrated, atmospheric water vapor transport. More specifically,

$$C = -\nabla \bullet \mathbf{Q}, \tag{3}$$

where

$$\mathbf{Q} = \frac{1}{g}\int_0^{\mathrm{p_{sfc}}} \mathbf{V}\mathrm{q}\mathrm{dp}, \tag{4}$$

and $\mathbf{V}$ is horizontal wind. The large-scale, vertically integrated budget equation for water in the ground and on the surface is (Schaake 1990)

$$\frac{\partial W}{\partial t} = (P - E) - S, \tag{5}$$

where W is a general term including both surface and subsurface liquid and frozen water, and S is the horizontal divergence of water flowing in the ground or at the surface. Combining (1) and (5) gives for the entire ground–atmosphere column

$$\frac{\partial P_W}{\partial t} + \frac{\partial W}{\partial t} = C - S. \tag{6}$$

On long timescales, such as several years, the storage becomes small and the terms on the right side of (6) should balance, that is,

$$\overline{C} = \overline{S}, \tag{7}$$

where the overbar refers to a long-term average. For shorter time periods, water storage, especially at and below the surface, may play a significant role in (6) and affect the relationship between *C* and *S*. For example, storage could cause a pulse input of water through convergence to appear as a delayed and temporally dispersed response in the streamflow (Freeze 1972).

We compare *C* and *S* for two river basins described later, for which *C* is computed from the NCEP reanalysis output. For *S*, we assume that subterranean groundwater losses and human water diversion from a region are negligible (cf. Roads et al. 1994). Under this assumption, *S* is then streamflow divergence, which we compute from river discharge records. We examine the degree to which (7) holds in the long-term average of our analysis data. We also note that streamflow in the United States generally reflects the variability of climate-forcing elements, such as atmospheric transport, precipitation, and temperature, by exhibiting a strong seasonal variation in the mean streamflow (Guetter and Georgakakos 1993). Thus we also examine the degree to which variability in atmospheric convergence corresponds with variability in streamflow divergence.

b. Analysis basins

In order to compare atmospheric water vapor convergence derived from the NCEP reanalysis with observed river discharge, or streamflow divergence, we defined two study basins according to the following criteria.

1) The basin must be large enough to contain many grid points of the NCEP reanalysis model.
2) The basin must have a no permanent snow or ice reservoirs.
3) The basin must have a single river-outflow point.

The first criterion is to ensure adequate resolution. The second criterion allows us to ignore potential interannual storage of water in snow and ice reservoirs. The third helps to reduce the possibility of significant unrecorded streamflow from the basin. On the basis of these criteria, two study basins were defined: the Upper Mississippi River Basin and the Ohio–Tennessee River Basin (Fig. 1). The transform grid of the data assimilation's spectral prediction model gives an approximate spatial resolution of the reanalysis (cf. Jarraud et al. 1981). On this basis, the Upper Mississippi Basin is resolved by 23 NCEP model grid points inside or within 1° of its border and the Ohio–Tennessee is similarly resolved by 25 grid points.

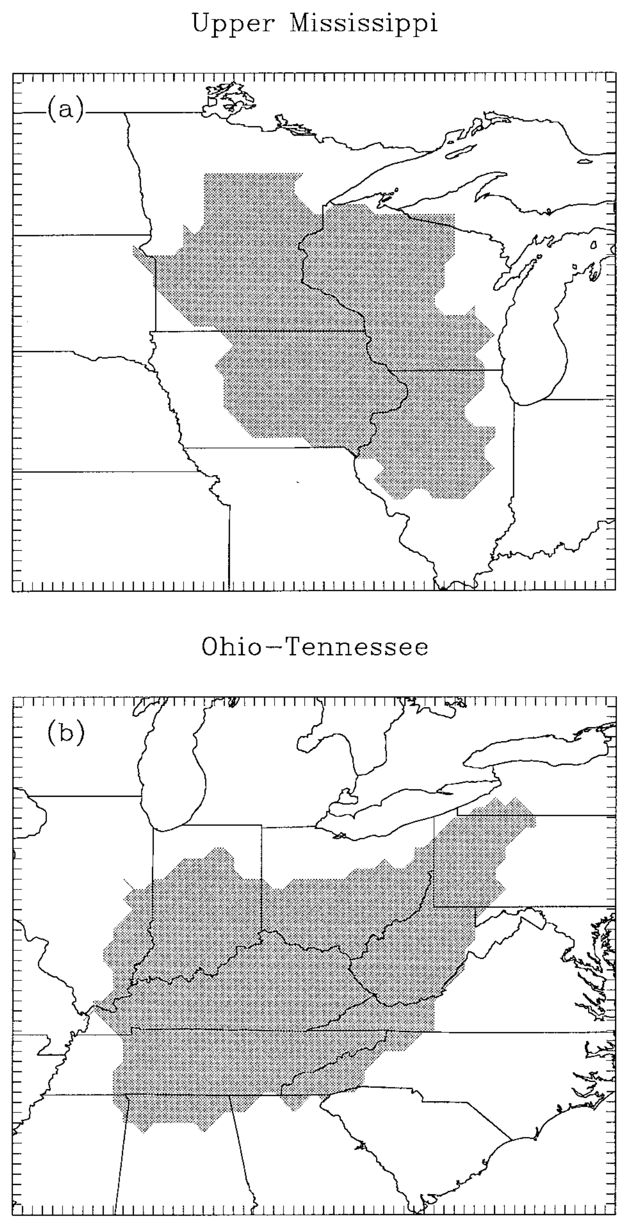

FIG. 1. The (a) Upper Mississippi and (b) Ohio–Tennessee Basins (shaded regions).

The Upper Mississippi River Basin covers parts of the five-state region of Illinois, Iowa, Minnesota, South Dakota, and Wisconsin, and includes the Upper Mississippi River and its major regional tributaries, such as the Black River, Cedar River, Des Moines River, Flambeau River, Illinois River, Iowa River, Minnesota River, Rock River, and Wisconsin River. Although the basin has a single river-outflow point, the distribution of operational stream-gauging stations forces us to estimate discharge from the Upper Mississippi River Basin as the sum of observed discharge for three subbasins: the Upper Mississippi River itself, measured at Keokuk, Iowa; the Des Moines River Basin, measured at Keosauqua, Iowa; and the Illinois River Basin, measured at Valley City, Illinois (Table 1). Keosauqua, Iowa, and Valley City, Illinois, are close to the outlets of their respective rivers. We define the outflow point of the basin as the confluence of the Illinois and Mississippi Rivers but ignore the small area of the basin so defined that is downstream from the measurement stations.

The Ohio–Tennessee River Basin covers parts of the 14-state region of Alabama, Georgia, Illinois, Indiana, Kentucky, Maryland, Mississippi, New York, North Carolina, Ohio, Pennsylvania, Tennessee, Virginia, and West Virginia. It includes the Ohio River, the Tennessee River, and their major regional tributaries, such as the Cumberland River, Green River, Holston River, Wabash River, and White River. Discharge for the basin is measured at Metropolis, Illinois (Table 1), near its outlet into the Mississippi River.

c. Data

Our analysis records cover the 10-yr period 1984–93. The NCEP reanalysis outputs used here are surface pressure and the horizontal wind and specific humidity computed for the 28 sigma layers of the reanalysis scheme's underlying forecast model. Data assimilation is performed by NCEP using a three-dimensional variational analysis scheme in which analysis variables are closely related to the sigma-coordinate spectral coefficients of the prognostic variables in the forecast model (Parrish and Derber 1992; Derber et al. 1991). The assimilation aims at preserving the dynamical consistency of mass and momentum fields. Water vapor is analyzed separately from the mass and momentum variables. By using sigma-layer output as opposed to output on standard pressure levels, we can compute directly the vertically integrated water transport as produced by the reanalysis scheme for its forecast model. We also then avoid errors described by Trenberth (1991) that can occur when the analysis output is interpolated and extrapolated to standard pressure levels. Note, however, that by using sigma-layer output, we are working with surface topography at the resolution (T62) used by the reanalysis model. The basins for which we compute atmospheric water vapor convergence have relatively small topographic variation, so differences between model and actual topography should be small and give only minor contributions to differences between reanalysis and actual water transport.

All fields are available four times daily (0000, 0600, 1200, and 1800 UTC) on an approximately 1.9° lat × 1.9° long Gaussian grid (Kalnay et al. 1996). At each point, we computed the vertical integral for (4) by assuming output fields are sigma-layer averages and summing over the layers. The output's Gaussian grid is highly suited for spectral transformation, so gridpoint quantities were transformed to spherical

TABLE 1. Streamflow-gauging stations used in this study and basin drainage areas (data source: http://h2o.usgs.gov).

USGS station number	Station name	Latitude	Longitude	Drainage area (km^2)
Upper Mississippi River Basin				409 039
05474500	Mississippi River at Keokuk	40°23′37″	91°22′27″	304 640
05490500	Des Moines River at Keosauqua	40°43′40″	91°57′34″	35 937
05586100	Illinois River at Valley City	39°42′12″	90°38′46″	68 462
Ohio–Tennessee River Basin				
03611500	Ohio River at Metropolis	37°85′10″	88°44′27″	525 770

harmonics at the resolution of the NCEP reanalysis model (T62), mainly to calculate derivatives but also to truncate product fields at T62 resolution.

The spectral transformation was also used to satisfy another purpose, computing water vapor convergence for the irregularly shaped basins. To perform this computation, we transformed the spectral components of water vapor convergence back to gridpoint values centered in $0.25° \times 0.25°$ cells. The actual resolution of the reanalysis data, of course, is still approximately $1.9° \times 1.9°$; the finer grid was used simply to match the spectral fields to the shapes of the river basins. Over the selected region, the gridpoint values were multiplied by their respective cell areas and summed. A gridpoint value along the basin boundary was included only if at least half of its area was within the basin. The integrated water vapor convergence was then divided by the area of the basin, giving an estimate of average amount per unit area. We performed test computations using cell sizes ranging from $2.5° \times 2.5°$ to $0.125° \times 0.125°$. Computed convergence was virtually the same for quarter-degree and smaller cells. Thus, for the Upper Mississippi River Basin, the atmospheric water vapor convergence is computed by summing over 732 quarter-degree cells covering 409 180 km^2; for the Ohio–Tennessee River Basin, convergence is computed using 867 quarter-degree cells covering an area of 526 200 km^2 (cf. Table 1).

Streamflow (discharge) records are abundant in the United States. The data employed in this study are from U.S. Geological Survey (USGS) daily streamflow records. As with the atmospheric data, the net streamflow out of a basin was divided by the basin's area to give an estimate of average streamflow divergence per unit area. For one of our observing stations, Keokuk, Iowa, river discharge was determined by the USGS from records of turbine and spillway gate operation at a power plant located in a dam across the Mississippi River (Southard et al. 1994). For the others, river discharge was derived by the USGS from stage height data using empirical relations between stage and discharge (Wahl et al. 1995).

The stage–discharge relation for a specific stream location is obtained from periodic discharge measurements made at known stages. The accuracy of streamflow thus depends on the stability of the stage–discharge relation and the accuracy of discharge measurements used to develop the relation (Roden 1967). Ice and snow can produce large changes in stage–discharge relations, potentially causing the relations to vary dramatically with time (Wahl et al. 1995). However, Winter (1981) estimated that the measurement uncertainty for long-term average values of streamflow at gauging station is around 5%. Generally, errors in daily values across the United States are less than 10% (e.g., Rasmusson 1968). For our three stations using stage–discharge relationships (Keosauqua, Valley City, Metropolis) hydrologic-year summaries (e.g., Southard et al. 1994; Zuehls et al. 1994) give estimates of the quality of the observations that are consistent with this general error estimate. For the calendar-year period 1984–93, the summaries indicate that over 85% of all daily records are considered accurate to within 15%, and over 70% of all daily records are considered accurate to within 10%. Records falling outside the 15% accuracy limit are generally estimated discharge amounts with unspecified error. Such records occur throughout the year with some concentration in winter. We assume that these records do not contaminate seriously our time series of streamflow divergence.

No accuracy assessment is provided with the Keokuk records. For this site, the USGS reviews the records provided by the Keokuk power company, makes a few check measurements, and publishes the data if it looks acceptable (W. Kirby 1996, personal communication). We assume that the accuracy of Keokuk data is comparable to the other three sites.

As noted earlier, we assume that human water diversion into or out of either of our basins is negligible. The annual records for Valley City state that its measurements include water diverted into the Illinois River from Lake Michigan through the Chicago Sanitary and Ship Canal at Lockport, Illinois. The annual average diversion is limited by U.S. Supreme Court decree to 90.6 m^3 s^{-1} (USGS 1980; Sullivan et al. 1990). Assuming the limit is attained every year, this diversion amounts to less than 3% of the discharge we compute for our Upper Mississippi Basin. Because the actual amount of daily diversion is not contained in the USGS records available to us, we have not attempted to correct the Valley City observations for this diversion. Records for the other stations we use do not indicate any human diversion for the study period.

3. Results

a. Time average

Table 2 shows the 10-yr average streamflow divergence and atmospheric water vapor convergence for the two study basins. The two streamflow di-

TABLE 2. Time-average streamflow divergence and water vapor convergence for the two study basins. Convergence is shown using output at all times available and using 0000 and 1200 UTC output only. Units are mm month^{-1}.

Basin	Streamflow divergence	Water vapor convergence (all times)	Water vapor convergence (0000 and 1200 UTC)
Upper Mississippi	21.8	30.5	18.9
Ohio–Tennessee	40.4	27.1	25.4

vergence values are larger than the U.S. average value of 17.5 mm month^{-1} obtained by Guetter and Georgakakos (1993) for the period 1939–88, indicating that each basin has a relatively strong throughput of water and thus plays an important role in the hydrologic cycle of the coterminous United States. Over a 10-yr period, we might expect the storage terms in (6) to be small so that (7) holds. However, in the Upper Mississippi River Basin, the time-average atmospheric convergence is 40% larger than its corresponding streamflow divergence, and in the Ohio–Tennessee River Basin, the convergence is 33% smaller than the divergence. The biases are comparable in magnitude to those found by Roads et al. (1994) for the United States and for the Mississippi Basin as a whole when using operational atmospheric analyses. Temporal variability statistics presented below will suggest that this disparity is not due to substantial water storage. Because long-term averages in river discharge appear to have errors of only a few percent (Winter 1981), the disparity would appear to be due to uncertainties in determining accurately the regional, atmospheric water vapor transport.

The reanalysis output is available every 6 h, but routine upper-air observations over the United States by rawinsondes occur only at 0000 and 1200 UTC. For the intermediate times 0600 and 1800 UTC, atmospheric water vapor convergence in the reanalysis may be strongly governed by the behavior of the numerical prediction model used for NCEP data assimilation. Substantial spinup in this model's hydrologic cycle could introduce a bias into the atmospheric water vapor convergence. To check for this bias, we computed the 10-yr average convergence for both basins using only 0000 and 1200 UTC output (Table 2). The imbalance in the Ohio–Tennessee Basin is slightly larger, but the imbalance in the Upper Mississippi Basin is considerably reduced. We have also examined the diurnal cycle of water vapor convergence into the Upper Mississippi during summer months, computing time-average convergent transport for each of the four daily analysis times. Plots of this transport (not shown) have large convergence into the Upper Mississippi Basin at 0600 UTC, which is close to the typical time of maximum strength of the nocturnal low-level jet (Bonner 1968; Mitchell et al. 1995; Higgins et al. 1996) that transports substantial amounts of water from the Gulf of Mexico up the Mississippi River Valley. Thus, the approximate balance of C with S in the Upper Mississippi Basin when using only 0000 and 1200 UTC output seems fortuitous and a consequence of high bias in the reanalysis convergence balancing low bias from neglect of water transport by the low-level jet. The much smaller change in time-average C in the Ohio–Tennessee Basin when using only 0000 and 1200 UTC output is consistent with the weaker influence of the nocturnal low-level jet in this basin. Equally important, the change in convergence when using only 0000 and 1200 UTC output shows the importance for the central United States of resolving adequately the diurnal cycle of transport. It is possible that even a four-times-daily analysis is not adequate in this regard, as Mitchell et al.'s (1995) climatology of the low-level jet shows substantial jet flow between 0600 and 1200 UTC that the analysis does not resolve. Indeed, work by Chen et al. (1996a) and Yarosh et al. (1997) indicates that atmospheric moisture budget studies in general require more frequent sampling or even continuous accumulation of atmospheric moisture convergence to depict accurately the moisture budget.

Despite the imbalances between C and S in Table 2, the time-average annual cycles of monthly atmospheric convergence and streamflow divergence (Fig. 2) do show physical consistency, though more so in the Ohio–Tennessee than Upper Mississippi Basin. Both basins experience their most substantial water gain during the cold half of the year (October–March), consistent with the 7-yr analysis of the water cycle for entire Mississippi Basin by Roads et al. (1994). Furthermore, the basin with the much larger annual-cycle amplitude in atmospheric convergence (Ohio–Tennessee) is also the basin with the much larger annual-cycle amplitude in streamflow divergence. In addition, the spring maximum in streamflow divergence for each basin lags the winter–spring maxima in atmospheric convergence, suggestive of a system where much water is stored as snow and ice in winter and released during spring thaw. In contrast, the Upper Mississippi's late autumn maximum in atmospheric convergence does not appear to have any lagged increase in streamflow divergence associated with it, perhaps raising reservations on the accuracy of this portion of the basin's annual cycle. In the cold half of the year, the annual cycle of atmospheric convergence is characterized by two maxima with a distinct midwinter minimum. During this part of the year, transient eddies are the primary contributors to extratropical, poleward moisture transport (Oort 1983). An examination of monthly latitude–longitude plots of meridional, transient-eddy heat fluxes in Oort's (1983) climatology indicates that the Upper Mississippi Basin is within the region of strong and frequent transient eddies (i.e., synoptic storms) during autumn and spring, but that transient eddies tend to pass to the south of the Upper Mississippi during midwinter. The midwinter minimum in C for the Upper Mississippi thus appears to be a real behavior resulting from seasonal changes in storm tracks, though the magnitude of the late autumn maximum in C appears overly strong relative to streamflow in early winter.

b. *Temporal evolution*

Figure 3 shows the 10-yr time series of seasonal-average streamflow divergence and water vapor convergence for two basins. Here, the seasons have their standard meteorological definitions: December–February for winter, March–May for spring, June–August for summer, and September–November for

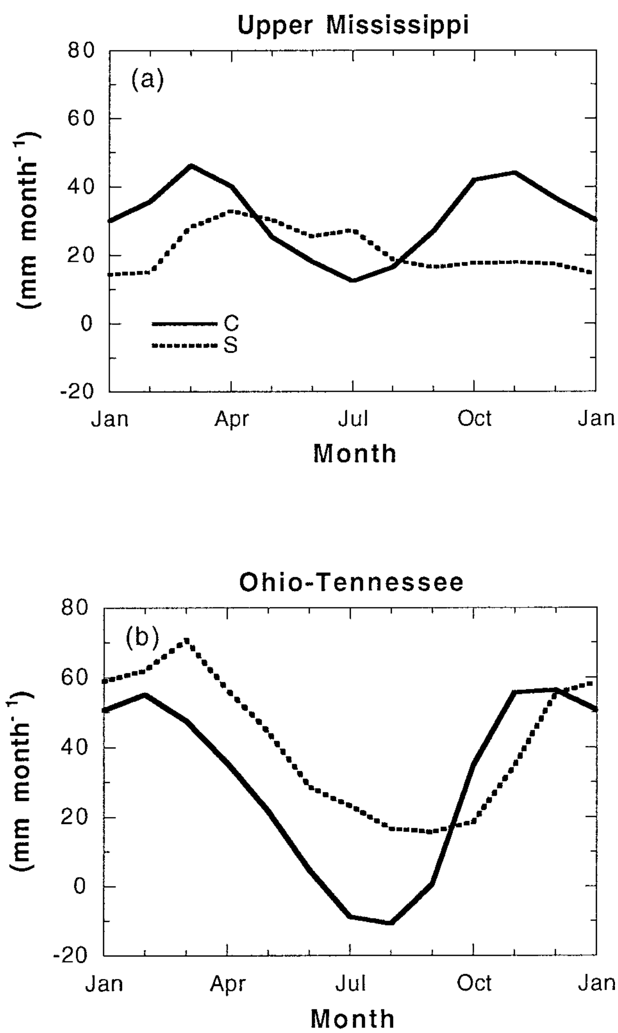

FIG. 2. Ten-year-average annual cycles of monthly atmospheric convergence, C, and streamflow divergence, S, for the (a) Upper Mississippi and (b) Ohio–Tennessee Basins.

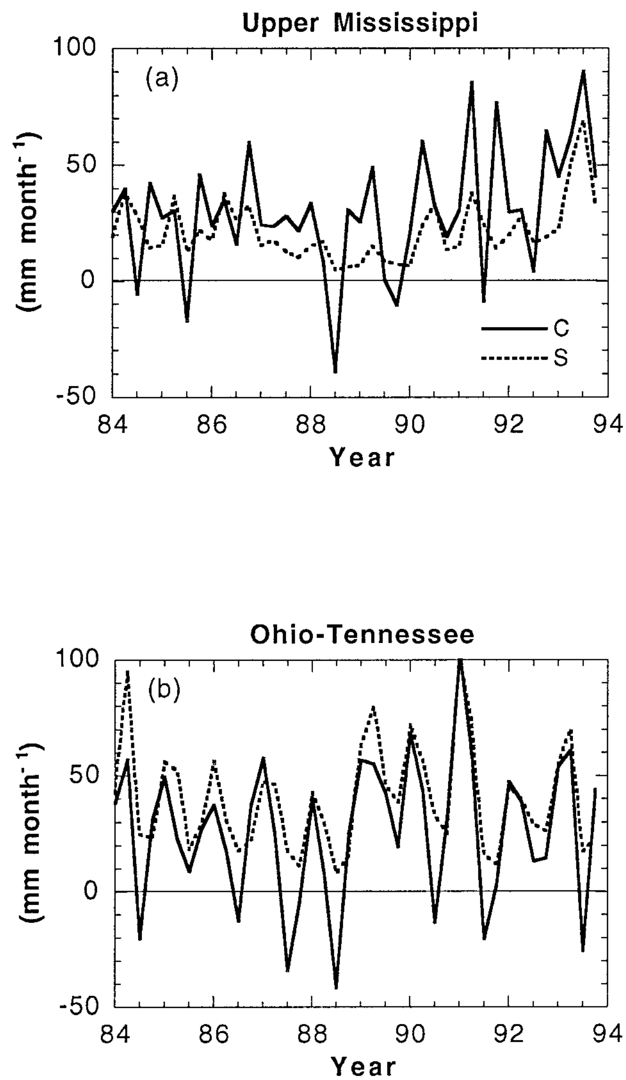

FIG. 3. Time series of seasonal-average atmospheric convergence, C, and streamflow divergence, S, for the (a) Upper Mississippi and (b) Ohio–Tennessee Basins.

autumn. For both basins, but especially the Ohio–Tennessee, larger atmospheric convergence is associated with larger streamflow divergence. Anomalous behavior in the Upper Mississippi associated with the 1988 drought and the 1993 flood appear in both time series. Also, summer is often a time of atmospheric water *divergence* from these basins, consistent with rawinsonde analysis of atmospheric water transport computed by C. Ropelewski and E. Yarosh (1997, manuscript submitted to *J. Climate*) for the central United States. Finally, the prominent annual cycle of streamflow divergence in the Ohio–Tennessee Basin indicates a relatively rapid flow of water through the complete land–atmosphere system comprising the basin. This behavior suggests that, at least for this basin, long-term water storage in the basin is not the reason for the imbalance between *C* and *S* in Table 2.

Figure 3 indicates a correlation, R, between atmospheric convergence and streamflow divergence for both basins in their interannual variability. Using the time series in Fig. 3 with linear trends and annual cycles removed, we computed R(X,Y,δt), the correlation of time series X with time series Y when X leads Y by δt. Since 1993 is an extreme year, including that year at the end of the time series could distort the trend computation, so we computed linear trends using the 9-yr record 1984–92. We then removed the annual cycle from our detrended 10-yr record by subtracting the 1984–92 average values for each season of the year. We also determined the statistical significance of the correlations by computing a joint autocorrelation time, τ_J, which indicates the interval between statistically independent samples of the time series and which was used to determine the statistical significance of correlations between *C* and *S* in temporal variability. Details of out statistical procedures appear in the appendix.

Table 3 shows for each basin the correlation between *C* and *S* for interannual variability, the joint autocorrelation time, and the 99% confidence level that a correlation is different from zero. Both correlations are significantly different from zero, though less than 60% of the variance in one field has a linear association with the variance in the other field. Note also that the relatively short joint autocorrelation time implies little lagged correlation between the two seasonal time series, which was confirmed by direct computation: R(S,C,δt) quickly drops to statistically insignificant values when $|\delta t|$ becomes one season or longer, primarily because the autocorrelation of atmospheric convergence R(C,C,δt) drops rapidly to insignificant values for $|\delta t| \geq$ one season.

We also examined the relationship between streamflow divergence and water vapor convergence using time series of daily data. We computed daily atmospheric convergence by averaging observations at 0000, 0600, 1200, and 1800 UTC for a calendar day. Arguably, for the central United States, 0000 UTC belongs to the previous calendar day. However, as indicated above, the single most important analysis time for a given day in this region appears to be the typical time of maximum in the nocturnal low-level jet, 0600 UTC. In addition, streamflow measurement times may vary. These issues were discussed by Roads et al. (1994). Guided by their work, we subjected the daily time series to a 5-day moving average, in part to minimize timing problems. After this smoothing we proceeded as before, removing the 9-yr trend from the full 10-yr time series and then computing the 9-yr average for each day and subtracting the averages from their contributing days in the time series. For each basin, we then computed the lagged correlation R(S,C,δt) as well as autocorrelations for both fields. We determined statistical significance in a manner similar to that used for the seasonal time series (see the appendix).

Figure 4 shows the lag correlation R(S,C,δt), the autocorrelation R(S,S,δt), and the 99% confidence level for nonzero correlation, R*, at each individual lag. The autocorrelation for atmospheric water vapor convergence drops quickly to statistically insignificant values for $|\delta t|$ > 5 days and so is not plotted here. Streamflow autocorrelation shows rather different behavior in the two basins. Autocorrelation can be viewed as a measure of how rapidly a basin's water system responds to external stimuli, where the water system includes all surface, subsurface, and atmospheric processes within the basin. Large autocor-

TABLE 3. Correlation coefficients, R(S,C,0), between the interannual variability of water vapor convergence and streamflow divergence for the two study basins. Also shown are the estimated joint autocorrelation times, τ_J, and 99% confidence levels, R*, where Δt = one season.

Basin	R(S,C,0)	$\tau_J/\Delta t$	R*
Upper Mississippi	0.68	1.15	0.51
Ohio–Tennessee	0.76	1.22	0.53

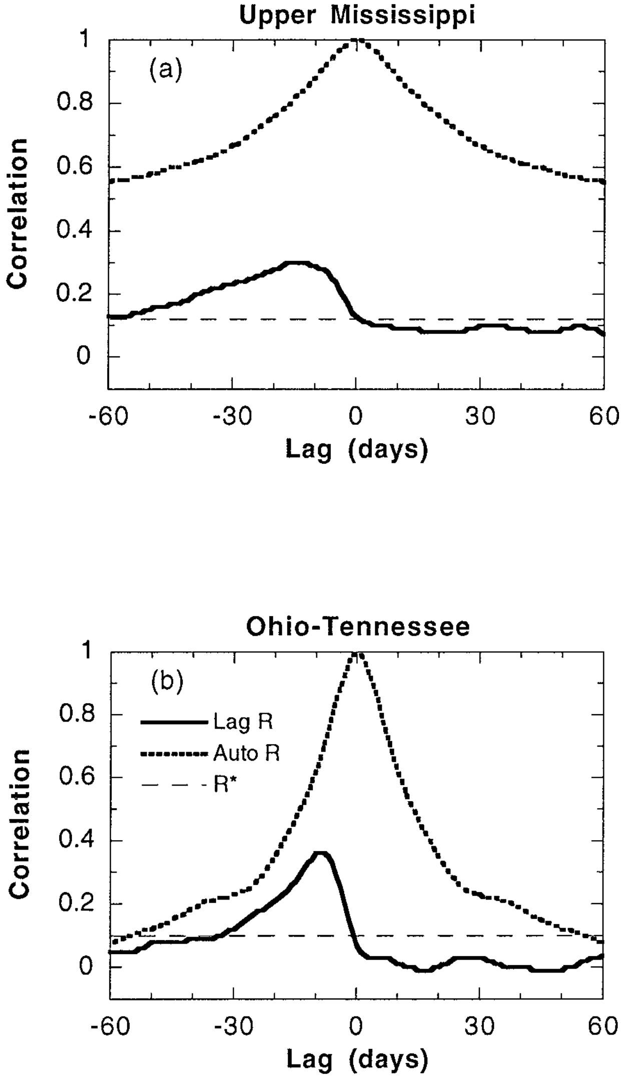

FIG. 4. The lag correlation R(S,C,δt), autocorrelation R(S,S,δt), and R* for daily time series in the (a) Upper Mississippi and (b) Ohio–Tennessee Basins. The key for all curves appears in (b).

relation at large lags implies that internal storage plays an important role in the basin's water cycle on the timescale of the lags (Dingman 1994), thus indicating a relatively sluggish or slowly responding system. Note that this storage could result from man-made control structures such as dams as well as from natural water reservoirs in the system, such as aquifers. On the basis of the streamflow autocorrelation function, the Ohio–Tennessee Basin is clearly a more rapidly responding system than the Upper Mississippi Basin, which has large autocorrelation even at lags of 60 days. This difference in daily responsiveness is consistent with the temporal variability of seasonal streamflow depicted in Fig. 3.

The lagged correlations between atmospheric convergence and streamflow divergence show statistically significant nonzero correlation for a span of days in which water vapor convergence leads streamflow divergence. This behavior is consistent with the physical expectation that atmospheric input ultimately yields streamflow output after the water works its way through regional reservoirs (natural and human). Processing of water through a regional aquifer–river system can be highly nonlinear (Freeze 1972), producing the type of temporally dispersed streamflow response to atmospheric input seen in Fig. 4. In addition, water can recycle between the land and atmosphere before flowing out (e.g., Brubaker et al. 1993), which would also contribute to a delay between atmospheric convergence and streamflow divergence. The correlations are similar to those computed in the study of Roads et al. (1994) for the entire Mississippi Basin, for which they found maximum correlation of about 0.30 for streamflow divergence lagging atmospheric convergence by 15–25 days. Maximum correlation occurs for shorter lag in the Ohio–Tennessee Basin than in the Upper Mississippi Basin, which is consistent with the more sluggish behavior of the latter implied in the streamflow autocorrelation. Despite the bias in the convergence time series relative to the streamflow time series, their joint temporal variability shows a behavior physically consistent with the streamflow autocorrelation.

In a similar manner, we computed R(S,C,δt), R(S,S,δt), and R* for each basin for each season (Figs. 5 and 6), where a season refers to the period covered by the atmospheric water vapor convergence data. Levels for significant nonzero correlation are now of course higher since the number of samples for any one season is only one-quarter of all the daily values. For both basins, but especially the Upper Mississippi, streamflow autocorrelation is greater in summer than winter, implying a greater role for storage on daily and weekly timescales in summer. For a central U.S. region that partially overlaps the Upper Mississippi, Brubaker et al. (1993) have found that water recycling between the land and atmosphere is greatest for the summer and autumn, which is when the largest lag correlations occur in Fig. 5, this indicating a physical consistency in the convergence–divergence relationship with other processes in the region. In addition, the Upper Mississippi experiences a greater annual cycle in the autocorrelation function. As with the complete time series in Fig. 4, the lag-giving maximum R(S,C,δt) tends to vary with season in a

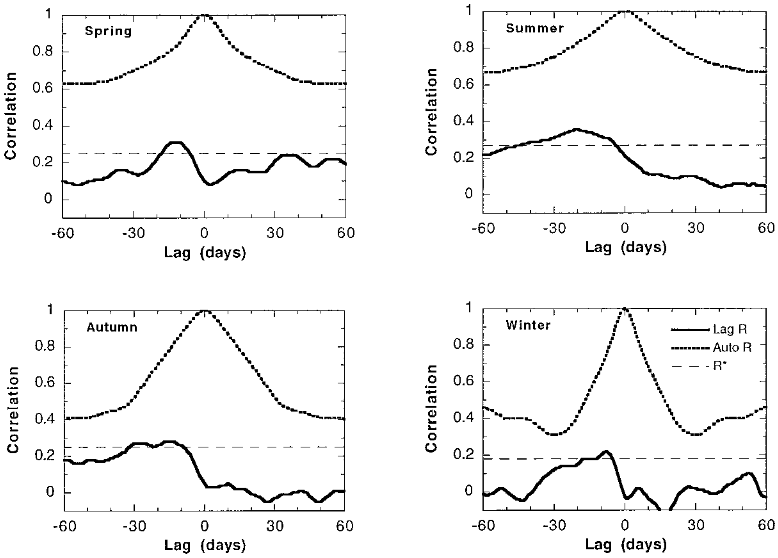

FIG. 5. As in Fig. 4 but for individual seasons in the Upper Mississippi Basin. The key for all curves appears in the winter panel.

manner consistent with the seasonal variation of streamflow autocorrelation. Again, this suggests a physical consistency in the lagged correlations between atmospheric convergence and streamflow divergence.

4. Summary and discussion

We have examined atmospheric water transport produced by the NCEP reanalysis for a 10-yr period, 1984–93. We compare transport convergence into a region with an independent dataset, river discharge or streamflow, and focus on two basins, the Upper Mississippi and the Ohio–Tennessee, where a relatively high density of routine, upper-air observations might be expected to give the reanalysis its closest rendition of the actual water transport. The two basins chosen are large enough to be reasonably well resolved by the data assimilation model. They also have no permanent snow and ice cover, which allows us to ignore potential interannual storage of water in snow and ice reservoirs, and a single outflow point, which helps to reduce the possibility of significant unrecorded streamflow from the basin.

Over periods of several years, the atmospheric convergence should match the water divergence from these basins in streamflow. However, we find an imbalance between the two with biases relative to streamflow approaching 40%. The accuracy attributed to river discharge measurements averaged over several years and the apparent lack of significant multiyear storage in the basins lead us to conclude that the bias is largely an inaccuracy in atmospheric transport, consistent with similar, previous analyses by Rasmusson (1968) and Roads et al. (1994). It is perhaps an encouraging trend that the biases observed here are comparable to these two earlier studies even though our study basins are smaller than the regions examined by those authors. Biases in the two basins examined are of opposite sign and if we combine the two basins, the net bias is only 11% with respect to streamflow divergence. It is conceivable that the bias in reanalysis convergence may become smaller as basin size increases, especially since a region's convergence will approach the true value of zero as the region is expanded to cover the entire globe. However, the balancing of errors here is more likely fortuitous since the two basins have only a short common border, in central Illinois (Fig. 1).

Subterranean flow into or out of these basins has been ignored in our study. The Great Lakes are in close proximity to

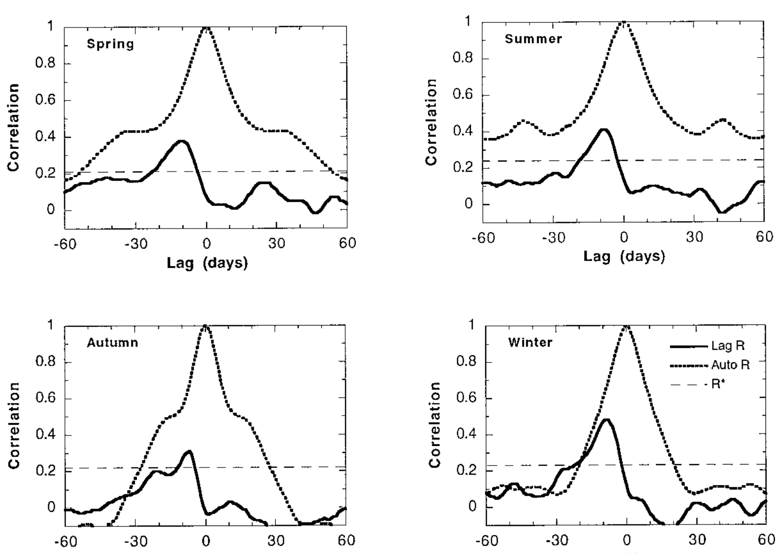

FIG. 6. As in Fig. 4 but for individual seasons in the Ohio–Tennessee Basin. The key for all curves appears in the winter panel.

both basins and could potentially interact with both through subterranean flow. On a continental scale, it appears that only a few percent of water flowing from the planet's landmasses to surrounding bodies of water is subterranean (Zektser and Loaiciga 1993). Estimating subterranean flow is difficult and to the best of our knowledge no such estimates exist for our study basins. If global data are a reasonable guide, then subterranean flow makes only a very small contribution to the disparity between time-average *C* and *S* in each of our study basins.

Temporal variability of the atmospheric convergence and streamflow divergence time series appears to show somewhat better correspondence. Statistically significant nonzero correlations occur for both basins on interannual and several-day timescales. The consistency of time-lagged correlations between *S* and *C* with the responsiveness of the basin's water cycle deduced from streamflow autocorrelation functions suggests that the lagged correlations are capturing actual physical behavior. The lagged correlation and streamflow autocorrelation functions using daily data for each basin show annual cycles, with both basins showing slower response times in summer. A possible explanation for the seasonal cycle is ground freezing in winter, which would reduce daily infiltration and storage of water in the soil. With reduced storage, the basin system would respond more rapidly to daily water input, thus reducing the lag between atmospheric convergence of water into the basin and the response of outflowing discharge. Soil freezing could also explain why the Upper Mississippi Basin has a stronger annual cycle in the δt for maximum R(S,C,δt) since it is located to the northwest of the Ohio–Tennessee Basin in a region of generally colder winter temperatures. Note that this explanation applies to the detrended daily data with annual cycle removed and so does not include the annual cycle of snow accumulation and melting evidently appearing in Fig. 2.

The results suggest that the temporal variability of water transport depicted by the reanalysis can be used, with some caution, to gain insight into the actual variability of atmospheric transport, at least for areas that are as well observed as the United States. The four-times-daily availability of the reanalysis appears to be the minimally acceptable frequency in regions like the Upper Mississippi Basin that are strongly affected by the water transport in the nocturnal low-level jet. The 0600 UTC analysis occurs near the typical time of maximum jet strength, but we cannot ascertain from this study whether or not additional time resolution is necessary to capture reasonably well the total transport into the basin by the low-level jet.

Acknowledgments. This research was supported in part by U.S. Department of Energy Grants DE-FG02-92ER61473 and DE-FG02-96ER61473 and U.S. National Science Foundation Grant ATM9123552. Additional support was provided by the Iowa Agriculture and Home Economics Experiment Station, Ames, Iowa, Project No. 3153, supported by Hatch Act and State of Iowa funds. We thank C.-F. Shih, D. Joseph, S. E. Jensen (NCAR), and M. Kanamitsu (NCEP) for their assistance in obtaining the reanalysis data; C. Lewis (National Water Data Exchange Office) for her assistance in obtaining the streamflow data; and W. Kirby (USGS) for answering our questions concerning streamflow observations and records. We also thank R. Arritt, T.-C. Chen, R. Rosen, E. Takle, C. Wikle, and the reviewers for comments; R. Turner for assistance in decoding and transforming the reanalysis data; and Mr. W. Jiang for graphics assistance. This is Journal Paper No. 17131 of the Iowa Agriculture and Home Economics Experiment Station, Ames, Iowa.

Appendix: Determination of Statistical Significance

We determined the statistical significance of the correlations by computing the joint autocorrelation time, τ_J, using (e.g., Stone et al. 1982)

$$\tau_J = \lim_{n\to\infty} \tau_n, \qquad \text{(A1)}$$

where

$$\frac{\tau_n}{\Delta t} = \sum_{i=-n}^{+n} R(C,C,i\Delta t)R(S,S,i\Delta t), \qquad \text{(A2)}$$

and R(X,Y,δt) is the correlation of time series X with time series Y when X leads Y by time period δt. In (A2), Δt = one season. For both basins, the sequence of τ_n (not shown) converged by n = 4 to their values in Table 3. For the seasonal-average time series, we then estimated the number of degrees of freedom (DF) using

$$\mathrm{DF} = \frac{(40\ \text{seasons})\Delta t}{\tau_J} - 3. \qquad \text{(A3)}$$

The 99% confidence level R* that a correlation is different from zero is given by a two-sided Student's t-test (e.g., Dingman 1994),

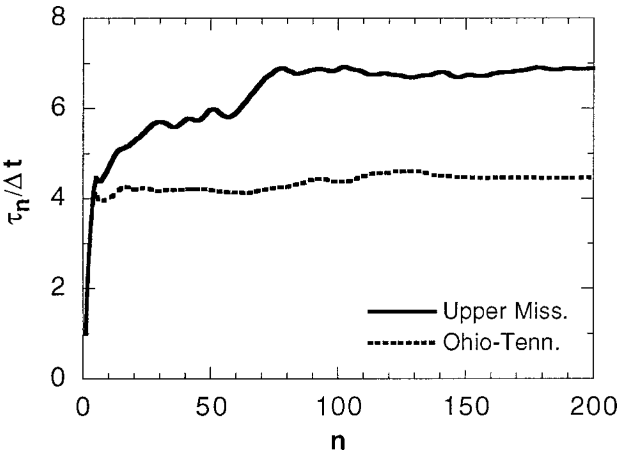

FIG. A1. The value of $\tau_n/\Delta t$ vs n for daily data in both basins.

$$R^* = \frac{2.85}{(DF)^{\frac{1}{2}}} \tag{A4}$$

For the daily time series, we again used (A1), (A2), and (A4), but now Δt = 1 day and

$$DF = \frac{N(\lambda)\Delta t}{\tau_J} - 3, \tag{A5}$$

where $N(\lambda)$ is the number of samples available for correlation computation at lag λ in our smoothed time series,

$$N(\lambda) = 3649 - \frac{\lambda}{\Delta t}. \tag{A6}$$

Figure A1 shows the sequence τ_n for our smoothed, detrended daily time series. For the Upper Mississippi Basin, we assume τ_J = 6.9 days, and for the Ohio–Tennessee Basin, we assume τ_J = 4.5 days; that is, the joint autocorrelation time is roughly the same as the window for our running average. For $\lambda = 0$, there are then 525 degrees of freedom in the Upper Mississippi River Basin's time series and 807 degrees of freedom in the Ohio–Tennessee River Basin's time series.

References

Bonner, W. D., 1968: Climatology of the low-level jet. *Mon. Wea. Rev.,* **96,** 833–850.

Brubaker, K. L., D. Entekhabi, and P. S. Eagleson, 1993: Estimation of continental precipitation recycling. *J. Climate,* **6,** 1077–1089.

Chahine, M. T., 1992: GEWEX: The global energy and water cycle experiment. *Eos, Trans. Amer. Geophys. Union,* **73,** 9.

Chen, S.-C., C. L. Norris, and J. O. Roads, 1996a: Balancing the atmospheric moisture budget. *J. Geophys. Res.,* **101,** 7341–7358.

Chen, T.-C., M.-C. Yen, and S. Schubert, 1996b: Hydrological processes associated with cyclone systems over United States. *Bull. Amer. Meteor. Soc.,* **77,** 1197–1205.

Derber, J. D., D. F. Parrish, and S. J. Lord, 1991: The new global operational analysis system at the National Meteorological Center. *Wea. Forecasting,* **6,** 538–547.

Dingman, S. L., 1994: *Physical Hydrology.* Macmillan College Publishing, 575 pp.

Donner, L. J., and P. J. Rasch, 1989: Cumulus initialization in a global model for numerical weather prediction. *Mon. Wea. Rev.,* **117,** 2654–2671.

Elliott, W. P., and D. J. Gaffen, 1991: On the utility of radiosonde humidity archives for climate studies. *Bull. Amer. Meteor. Soc.,* **72,** 1507–1520.

Freeze, R. A., 1972: Role of subsurface flow in generating surface runoff: 1. Baseflow contributions to channel flow. *Water Resour. Res.,* **8,** 609–623.

Guetter, A. K., and K. P. Georgakakos, 1993: River outflow of the coterminous United States, 1939–1988. *Bull. Amer. Meteor. Soc.,* **74,** 1873–1891.

Higgins, R. W., K. C. Mo, and S. D. Schubert, 1996: The moisture budget of the central United States as evaluated in the NCEP/NCAR and the NASA/DAO reanalyses. *Mon. Wea. Rev.,* **124,** 939–963.

Houze, R. A., and P. V. Hobbs, 1982: Organization and structure of precipitating cloud systems. *Advances in Geophysics,* Vol. 41, Academic Press, 3405–3411.

Iselin, J. P., and W. J. Gutowski. 1997: Water vapor layers in STORM-FEST rawinsonde observations. *Mon. Wea. Rev.,* **125,** 1954–1963.

Jarraud, M., C. Girard, and U. Cubasch, 1981: Comparison of medium range forecasts made with models using spectral or finite difference techniques in the horizontal. ECMWF Tech. Rep. No. 23, 96 pp. [Available from European Centre for Medium-Range Weather Forecasts, Shinfield Park, Reading, Berkshire RG29AX, United Kingdom.]

Kalnay, E., and R. Jenne, 1991: Summary of the NMC/NCAR reanalysis workshop of April 1991. *Bull. Amer. Meteor. Soc.,* **72,** 1897–1904.

——, and Coauthors, 1996: The NCEP/NCAR 40-year reanalysis project. *Bull. Amer. Meteor. Soc.,* **77,** 437–471.

Mitchell, M. J., R. W. Arritt, and K. Labas, 1995: A climatology of the warm season Great Plains low-level jet using wind profiler observations. *Wea. Forecasting,* **10,** 576–591.

National Research Council, 1991: *Opportunities in Hydrologic Sciences.* National Academy Press, 348 pp.

Oort, A. H., 1983: *Global Atmospheric Circulation Statistics, 1958–1973.* U.S. Department of Commerce, 180 pp.

Parrish, D. F., and J. C. Derber, 1992: The National Meteorological Center's spectral statistical interpolation analysis system. *Mon. Wea. Rev.,* **120,** 1747–1763.

Peixoto, J. P., and A. H. Oort, 1992: *Physics of Climate.* American Institute of Physics, 520 pp.

——, D. A. Salstein, and R. D. Rosen, 1981: Interannual variation in large-scale moisture fields. *J. Geophys. Res.,* **86,** 1255–1264.

Pratt, R. W., 1985: Review of radiosonde humidity and temperature errors. *J. Atmos. Oceanic Technol.,* **2,** 404–407.

Rasmusson, E. M., 1967: Atmospheric water vapor transport and the water balance of North America, Part I. Characteristics of the water vapor flux field. *Mon. Wea. Rev.,* **95,** 403–426.

——, 1968: Atmospheric water vapor transport and the water balance of North America, Part II. Large-scale water balance investigations. *Mon. Wea. Rev.,* **96,** 720–734.

Roads, J. O., S.-C. Chen, A. K. Guetter, and K. P. Georgakakos, 1994: Large-scale aspects of the United States hydrologic cycle. *Bull. Amer. Meteor. Soc.,* **75,** 1589–1610.

Roden, G. I., 1967: On river discharge into the northeastern Pacific Ocean and the Bering Sea. *J. Geophys. Res.,* **72,** 5613–5629.

Rosen, R. D., D. A. Salstein, and J. P. Peixoto, 1979a: Streamfunction analysis of interannual variability in large-scale water vapor flux. *Mon. Wea. Rev.,* **107,** 1682–1684.

——, ——, and ——, 1979b: Variability in the annual fields of large-scale atmospheric water vapor transport. *Mon. Wea. Rev.,* **107,** 26–37.

Savijarvi, H. I., 1988: Global energy and moisture budgets from rawinsonde data. *Mon. Wea. Rev.,* **116,** 417–430.

Schaake, J. C., 1990: From climate to flow. *Climate Change and United States Water Resources,* P. E. Waggoner, Ed., John Wiley and Sons, 177–206.

Southard, R. E., D. Sneck-Fahrer, C. J. Anderson, R. D. Goodrich, and J. G. Gorman, 1994: Water resources data—Iowa, water year 1993. Annual Report USGS-WDR-IA-93, U.S. Geological Survey, 388 pp. [NTIS PB94-196102XSP.]

Starr, D. O., and S. H. Melfi, 1991: The role of water vapor in climate: A strategic plan for the proposed GEWEX water vapor project (GVaP). NASA Conf. Publ. 3120, 50 pp. [Available from International GEWEX Program Office, 600 Maryland Ave., SW, Plaza Suite 1, Washington, DC 20024.]

Stone, P. H., S. J. Ghan, D. Spiegel, and S. Rambaldi, 1982: Short-term fluctuations in the eddy heat flux and baroclinic stability of the atmosphere. *J. Atmos. Sci.,* **39,** 1734–1746.

Sullivan, D. J., P. D. Hayes, T. E. Richards, and J. C. Maurer, 1990: Water resources data—Illinois, water year 1989, volume 2, Illinois River Basin. Annual Report USGS-WDR-IL-89-2, U.S. Geological Survey, 467 pp. [NTIS: PB90-230905XSP.]

Trenberth, K. E., 1991: Climate diagnostics from global analyses: Conservation of mass in ECMWF analyses. *J. Climate,* **4,** 707–722.

——, and C. J. Guillemot, 1995: Evaluation of the global atmospheric moisture budget as seen from analyses. *J. Climate,* **8,** 2239–2254.

USGS, 1980: Water resources data—Illinois, water year 1979, volume 2, Illinois River Basin. Annual Report USGS-WDR-IL-79-2, U.S. Geological Survey, 401 pp.

Wade, C. G., 1991: Improved low humidity measurements using the radiosonde hygristor. Preprints, *Seventh Symp. on Meteorological Observations and Instrumentation,* New Orleans, LA, Amer. Meteor. Soc., 285–290.

——, 1994: An evaluation of problems affecting the measurement of low relative humidity on the United States radiosonde. *J. Atmos. Oceanic Technol.,* **11,** 687–700.

Wahl, K. L., W. O. Thomas Jr., and R. M. Hirsch, 1995: The stream-gaging program of the U.S. Geological Survey. U.S. Geological Survey Circular 1123, 22 pp. [Available from U.S. Geological Survey, Information Services, Box 25286, Federal Center, Denver, CO 80225.]

Winter, T. C., 1981: Uncertainties in estimating the water balance of lakes. *Water Resour. Bull.,* **17,** 82–115.

Yarosh, E. S., C. F. Ropelewski, and E. Berbery, 1997: Observed water budgets over the GCIP domain: Role of diurnal variability and spatial sampling. Preprints, *13th Conf. on Hydrology,* Long Beach, CA, Amer. Meteor. Soc., 38–41.

Zektser, I. S., and H. A. Loaiciga, 1993: Groundwater fluxes in the global hydrologic cycle: Past, present and future. *J. Hydrol.,* **144,** 405–427.

Zuehls, E. E., J. K. La Tour, and T. L. Wicker, 1994: Water resources data—Illinois, water year 1993, volume 2, Illinois River Basin. Annual Report USGS-WDR-IL-93-2, U.S. Geological Survey, 297 pp. [NTIS PB94-204120XSP.]